Laser Radiation Pressure Slowing of a Molecular Beam

J. F. Barry, E. S. Shuman, E. B. Norrgard, and D. DeMille

Phys. Rev. Lett. **108**, 103002 — Published 8 March 2012

DOI: 10.1103/PhysRevLett.108.103002

Laser radiation pressure slowing of a molecular beam

J.F. Barry*, E.S. Shuman, E.B. Norrgard, and D. DeMille
Department of Physics, Yale University, P.O. Box 208120, New Haven, CT 06520, USA

We demonstrate deceleration of a beam of neutral strontium monofluoride (SrF) molecules using radiative forces. Under certain conditions, the deceleration results in a substantial flux of detected molecules with velocities $\lesssim 50\frac{m}{s}$. Simulations and other data indicate that the detection of molecules below this velocity is greatly diminished by transverse divergence from the beam. The observed slowing, from $\sim 140\frac{m}{s}$, corresponds to scattering $\gtrsim 10^4$ photons. We also observe longitudinal velocity compression under different conditions. Combined with molecular laser cooling techniques, this lays the groundwork to create slow and cold molecular beams suitable for trap loading.

PACS numbers: 37.10.Pq, 37.10.Mn, 37.10.Vz

There is substantial interest in producing samples of ultracold molecules for possible applications in quantum computation [1, 2], quantum simulation of condensed matter systems [3–5], precision measurements [6–11], controlled chemistry [12–14], and high precision spectroscopy [15]. A crucial step to obtaining large samples of ultracold, trapped molecules is developing a means to bridge the gap between typical molecular source velocities ($\sim 150-600\frac{m}{s}$) and velocities for which trap loading or confinement is possible ($\lesssim 5-20\frac{m}{s}$). Tremendous advances have been made in the deceleration of molecular beams in the past decade. Stark deceleration [16–19], Zeeman deceleration [20–22], counter-rotating nozzles [23, 24], collisional deceleration [25], and photodissociation [26] have all been demonstrated to slow molecular beams. However, only for fairly light species (~ 20 amu) with substantial vapor pressure at room temperature have these methods been demonstrated to allow slowing to velocities necessary to make trapping possible [27–30]. Optical deceleration has been demonstrated to slow molecular beams to rest [31, 32], but the high laser intensities required limit application to small volumes.

While these methods are useful, all of them conserve phase-space density and hence slow without cooling. However, recently it has been demonstrated that radiative forces can be used to cool molecules [33–36]. Assuming a given species is amenable to laser cooling, the same radiative forces can be used for slowing. As is well known from atoms [37, 38], laser slowing can be effective over broad velocity ranges and is insensitive to position, so that it can work on a large phase-space volume of molecules. Laser slowing can also lead to simultaneous longitudinal velocity compression, which is advantageous for loading traps. Once trapped, these molecules may be further laser-cooled to increase the phase-space density. Finally, laser slowing methods appear viable for a variety of species [11, 33, 34, 39–42], including some for which current phase-space-conserving slowing methods appear ill-suited; this is useful for addressing the needs of the variety of applications envisioned for ultracold molecules [43].

Here we experimentally demonstrate deceleration of a molecular beam by radiative forces. This work builds upon similar results demonstrating deflection [35] and transverse cooling [36] of a molecular beam by radiative forces. The crucial enabling feature for radiative slowing is the ability to scatter $\gtrsim 10^4$ photons without heating the internal degrees of freedom of the molecules. Our scheme for creating a quasi-cycling transition [35, 36] is recounted briefly here and depicted in Fig. 1. We employ the X $^2\Sigma^+_{1/2}(v{=}0, N{=}1) \rightarrow A\ ^2\Pi_{1/2}(v'{=}0, J'{=}1/2)$ electronic

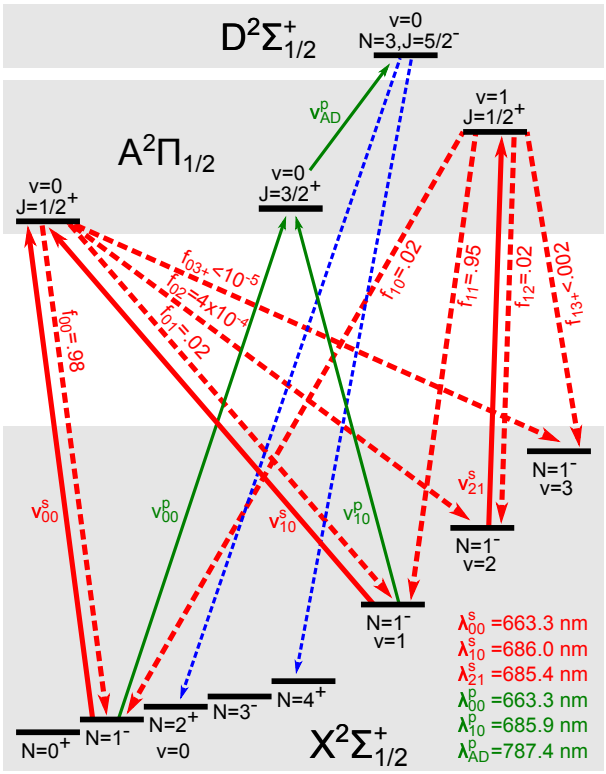

FIG. 1. (color online). **Relevant energy levels and transitions in SrF.** Solid thick red lines denote slowing lasers, while solid thin green lines denote probe lasers. Dashed thick red lines denote spontaneous decay channels from the A state and corresponding FCFs ($f_{v'v}$) are labeled. Dashed thin blue lines indicate decay fluorescence channels used to determine the beam Doppler profile.

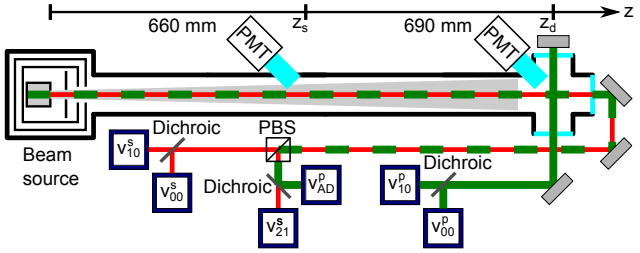

FIG. 2. (color online). **Schematic of the apparatus.** Thin red (thick green) lines indicate slowing (probe) laser beams. PMT locations are marked on the z axis.

transition of SrF, with $\tau = 24$ ns lifetime, for cycling and slowing. We denote by v^s_{00} the frequency of the main cycling and slowing laser, with wavelength λ^s_{00} and detuning from resonance Δv^s_{00}. The favorable Franck-Condon factors (FCFs) of SrF limit vibrational branching [33]. Separate repump lasers, denoted v^s_{10} and v^s_{21}, address residual vibrational leakage. Driving an $N{=}1{\rightarrow}J'{=}1/2$ transition eliminates rotational branching [34], while a magnetic field remixes the resulting dark ground-state Zeeman sublevels [44]. This scheme should allow $\gtrsim 10^5$ photon scattering cycles before the bright state population is reduced by $1/e$ [35, 36].

We use an ablation-loaded cryogenic buffer gas beam source, which provides relatively low initial forward velocities, low internal temperatures, and high brightness [45–50]. It produces an SrF molecular beam of $1.2{\times}10^{11}$ molecules/sr/pulse in the X $^2\Sigma^+_{1/2}(v{=}0, N{=}0)$ state. To mitigate variations of the molecular beam flux, data are taken by chopping the slowing lasers on or off between successive ablation shots. The background pressure in the beam propagation region is $\sim 2{\times}10^{-7}$ Torr.

With the v^s_{00}, v^s_{10}, and v^s_{21} lasers applied, molecules cycle over the three bright ground states: X($v{=}0, 1, 2; N{=}1$). The $X(v = 0, 1; N = 1)$ populations are expected to be comparable, while the X($v{=}2, N{=}1$) population should be significantly less since the FCFs dictate that decays to this latter state are rare compared to the rate at which population in this state is pumped out via the $A(v = 1, N = 1)$ intermediate state. We hence employ a scheme to detect population in both X($v{=}0, 1; N{=}1$) states (with resolved spin-rotation structure (SRS) and hyperfine structure (HFS)). These states are excited to the A($v{=}0, J{=}3/2$) state (unresolved HFS) via two perpendicular probe lasers, denoted v^p_{00} and v^p_{10}, which are spatially overlapped and intersect the molecular beam at $z{=}z_d$, 1350 mm downstream from the source, as shown in Fig. 2. A longitudinally propagating probe laser, denoted v^p_{AD}, then excites to the D($v = 0, N = 3, J = 5/2$) state (unresolved HFS), and the resulting laser-induced fluorescence (LIF), predominantly at 360 nm, is filtered and measured by a photon-counting PMT at $z{=}z_d$,. Monitoring the D$\rightarrow$X LIF as a function of the v^p_{AD} laser frequency yields a Doppler-shifted longitudinal velocity profile (LVP) free of SRS/HFS, at a wavelength easily filtered from all laser light. Both the v^p_{00} and v^p_{10} lasers have frequency-modulated (FM) sidebands with modulation frequency $f_{mod}{=}42$ MHz and modulation index $m{=}2.6$ to excite all SRS/HFS levels of the X($v{=}0, 1; N = 1$) states [35]; since they intersect the collimated molecular beam transversely, they are subject to negligible Doppler shift and broadening. The v^p_{00} and v^p_{10} laser powers are set to drive both transitions with the same Rabi frequency.

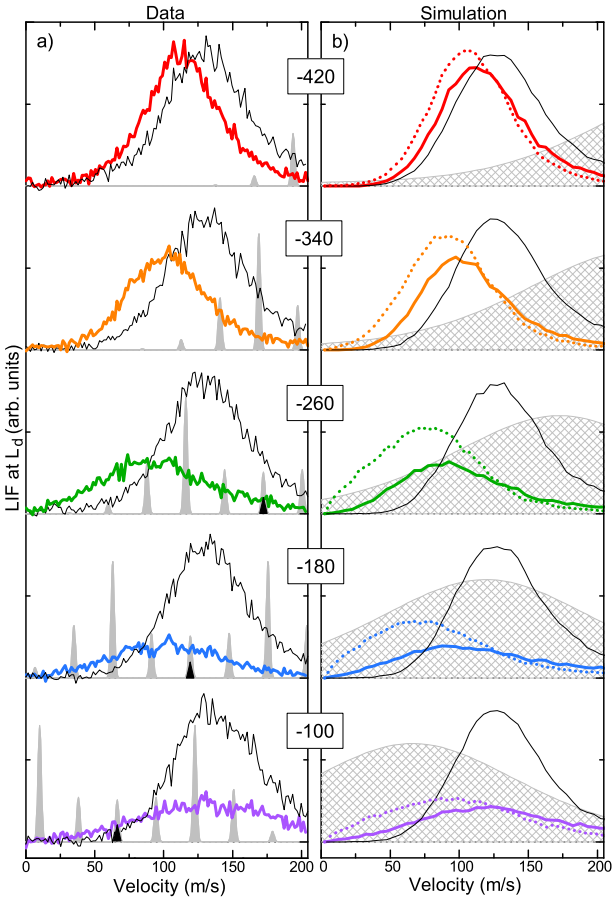

FIG. 3. (color online). **Measured and simulated slowing for different detunings of the main slowing laser.** a) Measured slowed LVP (solid thick color), control LVP (—), and velocities corresponding to the v^s_{00} FM sideband spectrum (gray, with center ▲). The panels are scaled so that all controls have equal heights. b) Simulated slowed LVP (solid thick color), simulated control LVP (—), and simulated slowed LVP with transverse cooling the entire length of the slowing region (dotted color, scaled by 1/21, the ratio of the peak heights of the simulated control LVPs without and with transverse cooling). The gray shaded area indicates the assumed force versus velocity profile used in the simulation. The Δv^s_{00} detuning (in MHz) is shown in the centered box for each panel set. The simulation indicates that not only does the addition of transverse cooling vastly increase the overall flux, but that the addition of transverse cooling should be effective in retaining the slowest molecules, which are most likely to be lost due to divergence.

We verified that the detection efficiency and measured LVP are independent of whether the molecule is detected from X(v=0, N=1) or X(v=1, N=1). Power broadening from the v^p_{AD} laser (∼23 MHz FWHM) and magnetic field broadening (∼18 MHz FWHM) lead to a measured broadening of 42 MHz FWHM for the v^p_{AD} detection profile, equivalent to all velocity profiles being convolved with a detection profile of 34 m/s FWHM.

The v^s_{00}, v^s_{10}, v^s_{21}, and v^p_{AD} lasers are spatially overlapped using a combination of dichroic mirrors and a polarizing beamsplitter (PBS) to produce a single beam with $\frac{1}{e^2}$ intensity waist d=3.4 mm (except for the v^p_{AD} laser with d=4.4 mm) counterpropagating to the molecular beam. To address all SRS/HFS levels over a wide velocity range, the v^s_{00}, v^s_{10}, and v^s_{21} lasers have FM sidebands with 41 MHz $< f_{mod} <$ 44 MHz and $m = 3.1$ unless noted otherwise. Due to the large frequency extent of the sidebands, we do not expect longitudinal velocity compression [51]. We note that the dark magnetic sublevels of the X($N = 1$) state prevent use of a Zeeman slower. The slowing lasers are not chirped [52] due to the temporal extent of the molecular beam pulse (∼10 ms). A supplementary light detector at z=z_s, 660 mm downstream from the source, allows monitoring of the LIF from spontaneously emitted photons during cycling. The v^s_{00}, v^s_{10}, v^s_{21} and v^p_{AD} laser powers are 140 mW, 73 mW, 45 mW, and 70 mW respectively. The v^s_{00}, v^s_{10}, and v^s_{21} laser detunings from resonance, denoted Δv^s_{00}, Δv^s_{10}, and Δv^s_{21} respectively, are first varied iteratively to maximize LIF at z=z_s. For finer tuning, the v^p_{AD} laser detuning from resonance, denoted Δv^p_{AD}, is set to resonantly excite SrF molecules with $v_f \approx 50\frac{m}{s}$, and Δv^s_{00}, Δv^s_{10}, and Δv^s_{21} are varied iteratively to maximize the number of molecules detected in that Doppler class. Unless explicitly noted, Δv^s_{10} and Δv^s_{21} remain at these empirically determined values, denoted $\Delta v^{s,opt}_{10}$ and $\Delta v^{s,opt}_{21}$ respectively. Magnetic field coils create an approximately uniform field B=9 G at an angle $\theta_B = 45°$ relative to the v^s_{00} linear polarization over the length 120 mm$\lesssim z \lesssim$1350 mm.

Application of the slowing lasers shifts the molecular beam LVP, as shown in Fig. 3a for various Δv^s_{00}. As Δv^s_{00} is tuned towards $\langle v_f\rangle/\lambda^s_{00}$ from the red (where $\langle v_f\rangle$ is the mean forward velocity), the LVP is shifted to lower velocities, until $\Delta v^s_{00} \approx \langle v_f\rangle/\lambda^s_{00}$ (i.e., when the slowing laser is tuned to the maximum of the Doppler-shifted peak); then, when tuned further to the blue, the LVP gradually returns to its unperturbed state. However, the shift to lower velocities is accompanied by a decrease in the number of detected molecules, which is most severe when $\Delta v^s_{00} \approx \langle v_f\rangle/\lambda^s_{00}$.

We use the quantity Δ_{HM}, defined as the shift of the half-maximum point on the leading edge of the observed slowed LVP (versus that of the control LVP), as one simple measure to evaluate the effectiveness of our slowing for different experimental parameters. Because slowed molecules are less likely to be detected (due to increased divergence, etc.), Δ_{HM} likely provides an underestimate of the actual slowing. With Δv^s_{00}=−260 MHz, providing resonant excitation for molecules with v_f=175$\frac{m}{s}$, we routinely achieve $\Delta_{HM} \approx 45-60\frac{m}{s}$. Since the SrF recoil velocity is v_{rc}=5.6$\frac{mm}{s}$, we interpret this as a mean number of photons scattered per molecule $\langle N_{sc}\rangle \approx 10^4$, roughly an order of magnitude greater than in previous work [36].

We argue that the decrease in the number of detected molecules is due primarily to increased divergence and transverse heating as the beam is slowed. Several other loss mechanisms were ruled out as the dominant cause after investigation. Increasing the background gas pressure (primarily helium) by 5× changed the slowed LVPs little, indicating that background gas collisions are not a dominant loss mechanism. We investigated possible loss to other rovibrational states which could arise from various mechanisms. For example, off-resonant excitation to the A(v=0, J=$\frac{3}{2}$) state by the v^s_{00} laser or HFS mixing in the A(v=0, J=$\frac{1}{2}$) state could transfer population to the dark X(v=0, N=3) state; stray electric fields could lead to decays from the A(v=0, J=$\frac{1}{2}$) state to the dark X(v=0; N=0, 2) states; or the v^p_{AD} laser could off-resonantly excite molecules from the A(v=0, J=$\frac{1}{2}$) state to the D(v=0, N=1) state before they reach z=z_d. To investigate such mechanisms, we explicitly probed the populations of the X(v=0; N=0, 2, 3) and X(v=1, N=0) states and determined that <10% combined total loss could be attributed to such processes. Loss to the X(v=3, N=1) state was not directly measured, but was estimated from the observed increase in spontaneous scattering LIF at $z = z_s$ by adding the v^s_{21} repump laser; this indicated that molecules cycled through the X(v=2, N=1) state ∼ 3× before reaching $z = z_d$. Together with the estimated FCFs [35], this yields an estimated ∼ 6% loss to the X(v=3, N=1) state. Over all, the inability to find evidence of population of dark states is preliminary evidence that our quasi-cycling transition is nearly closed for up to ∼10^4 scattered photons.

The decrease in the number of detected molecules due to increased divergence and transverse heating was modeled via a Monte Carlo simulation. In the simulation, particles are created at the source with randomized velocity distribution matching the measured forward and transverse velocity distributions of our source [45]. We assume equal detection efficiency over the v^p_{AD} $\frac{1}{e^2}$ beam waist at $z = z_d$. We estimate the force profile using a model 5-level system consisting of one excited state and four ground states (to match the four SRS/HFS levels). The degeneracy of the SRS/HFS levels and the accompanying level shifts and remixing within each SRS/HFS level due to the applied B-field are not included in the simulation. The saturation parameter s is calculated for each of the four SRS/HFS levels assuming an estimated saturation intensity of 6 mW/cm^2 and the known v^s_{00} laser FM sideband spectrum. Using τ and s, classical

rate equations are solved to determine the equilibrium excited state population fraction, ρ_{ee}, as a function of the laser detuning from the center of the Doppler shifted SRS/HFS spectrum, Δ. The dependence of ρ_{ee} is then fit to a Voigt profile. This process is repeated for the range of powers dictated by the v^s_{00} laser's Gaussian intensity profile. Using the peak values of ρ_{ee} for each intensity, we derive an estimate of how the maximum scattering rate varies with the distance from the center of the slowing beams, r. We finally model the scattering rate R as the analytic function

$$R(\Delta, r) = R_{max}\left[\frac{1}{1+(r/r_0)^a}\right]\left[N_1\int_{-\infty}^{\infty}\frac{e^{-t^2/(2w_G^2)}}{(w_L/2)^2+(\Delta-t)^2}dt\right],$$

where the normalization N_1 is chosen so that $R(0,0) = R_{max}$. The parameter values r_0=1.3 mm, a=3.75, w_L=99 MHz and w_G=95 MHz are derived from these fits, without reference to the LVP data. The first two parameters control how the scattering rate varies with the beam intensity, while the latter two characterize the functional dependence of R on Δ. Finally, the free parameter R_{max} is varied manually to fit the LVP data for a variety of Δ. We achieve good agreement with $R_{max} = 2.8 \times 10^6$ s^{-1}, consistent with our previous observations [35]. Typical simulation results, shown in Fig. 3b, indicate that nearly all of the decrease in the number of detected molecules can be attributed to increased divergence and transverse heating. According to the simulation, the addition of transverse cooling to counteract divergence losses can vastly increase the flux of slow molecules. Several other pieces of evidence (e.g., dependence of the slowed LVP on laser power for various detunings) suggest that larger scattering rates may result in greater slowing but that this additional slowing may not be apparent in the data due to increased divergence and therefore decreased detection probability for the slowest molecules.

Most data was taken with an ambient magnetic field of $B \approx 4-9$ G and $\theta_B = 45°$. Over this range, the slowed LVPs and LIF at $z=z_s$ were fairly insensitive to the value of B. However, we observed that Earth's magnetic field, $B_E \approx .5$ G with $\theta_B \approx 102°$, on its own allows some remixing of the dark Zeeman sublevels. Under certain conditions when $B = B_E$, qualitatively different behavior was observed; namely, sharp features appeared in the LVP, as shown in Fig. 4. Moreover, under these conditions there is clear evidence for longitudinal velocity compression: the ratio of peak height to width of the LVP increases under these conditions for certain detunings Δv^s_{00}. We have been unable to find a simple explanation for these features, and full modeling of the system (including all ∼33 slowing laser frequencies, 44 molecular sublevels, B-field remixing, coherent dark states [44], etc.) is beyond the scope of this paper. However, this behavior could potentially be used to compress the molecular beam LVP. Ideally this would be done after slowing had already removed most of the kinetic energy from the beam, e.g., by using an initial region of large B for broadband slowing, followed by a second region of small B for longitudinal velocity compression and further slowing. A slow and nearly monoenergetic beam would be ideal for trap loading.

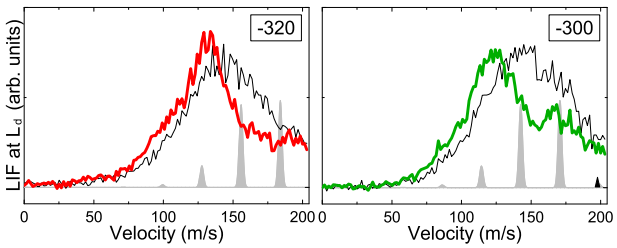

FIG. 4. (color online). **Slowing with no applied magnetic field.** The Δv^s_{00} detuning (in MHz) is shown in the upper right. Otherwise the representation is the same as in Fig. 3. Note the sharp features, in particular the increase in the ratio of peak height to width of the LVP; these indicate longitudinal velocity compression within part of the distribution. This should be contrasted with the smooth LVPs obtained at large B (Fig. 3). Here m=2.6 for the v^s_{00} laser, where the sharp features were generally more pronounced than at the typical $m = 3.1$ used for most of the slowing data.

In summary, we have demonstrated radiation pressure slowing of an SrF molecular beam. Under certain conditions, we detect ∼6% of the initial detected flux at velocities $<50\frac{m}{s}$. The dominant loss mechanism at present is the increased divergence and transverse heating of the beam due to the slowing. The addition of transverse cooling should provide a much higher flux of slow molecules, suitable for loading a trap. It may be possible to use a low B-field section to compress the velocity distribution following the initial slowing. A slow molecular beam could be directly loaded into either a magneto-optical trap (MOT) [34] or a sufficiently deep conservative trap, using optical pumping as a dissipative loading mechanism [53–59]. Furthermore, the preliminary evidence of little loss during cycling, even after $\gtrsim 10^4$ photons have been scattered, invites the possibility of moderately long lifetimes for SrF in a MOT.

This material is based upon work supported by the ARO, the NSF and the AFOSR under the MURI award FA9550-09-1-0588.

[1] D. DeMille, Phys. Rev. Lett. **88**, 067901 (2002).
[2] A. André, D. DeMille, J. M. Doyle, M. D. Lukin, S. E. Maxwell, P. Rabl, R. J. Schoelkopf, and P. Zoller, Nature Phys. **2**, 636 (2006).
[3] K. Goral, L. Santos, and M. Lewenstein, Phys. Rev. Lett. **88**, 170406 (2002).
[4] A. Micheli, G. K. Brennen, and P. Zoller, Nature Phys. **2**, 341 (2006).

[5] R. Barnett, D. Petrov, M. Lukin, and E. Demler, Phys. Rev. Lett. **96**, 190401 (2006).
[6] J. J. Hudson, B. E. Sauer, M. R. Tarbutt, and E. A. Hinds, Phys. Rev. Lett. **89**, 023003 (2002).
[7] J. J. Hudson, D. M. Kara, I. J. Smallman, B. E. Sauer, M. R. Tarbutt, and E. A. Hinds, Nature **473**, 493 (2011).
[8] D. DeMille, S. B. Cahn, D. Murphree, D. A. Rahmlow, and M. G. Kozlov, Phys. Rev. Lett. **100**, 023003 (2008).
[9] A. C. Vutha, W. C. Campbell, Y. V. Gurevich, N. R. Hutzler, M. Parsons, D. Patterson, E. Petrik, B. Spaun, J. M. Doyle, G. Gabrielse, and D. DeMille, J. Phys. B: At. Mol. Opt. Phys. **43**, 074007 (2010).
[10] A. Leanhardt, J. Bohn, H. Loh, P. Maletinsky, E. Meyer, L. Sinclair, R. Stutz, and E. Cornell, J. Mol. Spec. **270**, 1 (2011).
[11] T. A. Isaev, S. Hoekstra, and R. Berger, Phys. Rev. A **82**, 052521 (2010).
[12] N. Balakrishnan and A. Dalgarno, Chem. Phys. Lett. **341**, 652 (2001).
[13] R. V. Krems, Phys. Chem. Chem. Phys. **10**, 4079 (2008).
[14] E. R. Hudson, C. Ticknor, B. C. Sawyer, C. A. Taatjes, H. J. Lewandowski, J. R. Bochinski, J. L. Bohn, and J. Ye, Phys. Rev. A **73**, 063404 (2006).
[15] V. V. Flambaum and M. G. Kozlov, Phys. Rev. Lett. **99**, 150801 (2007).
[16] H. L. Bethlem, G. Berden, and G. Meijer, Phys. Rev. Lett. **83**, 1558 (1999).
[17] S. Y. T. van de Meerakker, P. H. M. Smeets, N. Vanhaecke, R. T. Jongma, and G. Meijer, Phys. Rev. Lett. **94**, 023004 (2005).
[18] E. R. Hudson, H. J. Lewandowski, B. C. Sawyer, and J. Ye, Phys. Rev. Lett. **96**, 143004 (2006).
[19] A. Osterwalder, S. A. Meek, G. Hammer, H. Haak, and G. Meijer, Phys. Rev. A **81**, 051401 (2010).
[20] N. Vanhaecke, U. Meier, M. Andrist, B. H. Meier, and F. Merkt, Phys. Rev. A **75**, 031402 (2007).
[21] E. Narevicius, A. Libson, C. G. Parthey, I. Chavez, J. Narevicius, U. Even, and M. G. Raizen, Phys. Rev. Lett. **100**, 093003 (2008).
[22] E. Narevicius, A. Libson, C. G. Parthey, I. Chavez, J. Narevicius, U. Even, and M. G. Raizen, Phys. Rev. A **77**, 051401 (2008).
[23] M. Gupta and D. Herschbach, J. Phys. Chem. A **103**, 10670 (1999).
[24] M. Strebel, F. Stienkemeier, and M. Mudrich, Phys. Rev. A **81**, 033409 (2010).
[25] M. S. Elioff, J. J. Valentini, and D. W. Chandler, Science **302**, 1940 (2003).
[26] A. Trottier, D. Carty, and E. Wrede, Mol. Phys. **109**, 725 (2011).
[27] G. Meijer, S. Y. T. van de Meerakker, and H. L. Bethlem, in *Cold Molecules: Theory, Experiment, Applications*, edited by R. V. Krems, W. C. Stwalley, and B. Friedrich (CRC Press, Boca Raton, 2009) pp. 509–552.
[28] M. R. Tarbutt, H. L. Bethlem, J. J. Hudson, V. L. Ryabov, V. A. Ryzhov, B. E. Sauer, G. Meijer, and E. A. Hinds, Phys. Rev. Lett. **92**, 173002 (2004).
[29] T. E. Wall, J. F. Kanem, J. M. Dyne, J. J. Hudson, B. E. Sauer, E. A. Hinds, and M. R. Tarbutt, Phys. Chem. Chem. Phys. **131**, 18991 (2011).
[30] J. E. van den Berg, S. Hoekman Turkesteen, E. B. Prinsen, and S. Hoekstra, ArXiv e-prints (2011), arXiv:1104.4328 [physics.atom-ph].
[31] R. Fulton, A. I. Bishop, and P. F. Barker, Phys. Rev. Lett. **93**, 243004 (2004).
[32] A. I. Bishop, L. Wang, and P. F. Barker, New J. Phys. **12**, 073028 (2010).
[33] M. D. Di Rosa, Eur. Phys. J. D **31**, 395 (2004).
[34] B. K. Stuhl, B. C. Sawyer, D. Wang, and J. Ye, Phys. Rev. Lett. **101**, 243002 (2008).
[35] E. S. Shuman, J. F. Barry, D. R. Glenn, and D. DeMille, Phys. Rev. Lett. **103**, 223001 (2009).
[36] E. S. Shuman, J. F. Barry, and D. DeMille, Nature **467**, 820 (2010).
[37] W. D. Phillips and H. Metcalf, Phys. Rev. Lett. **48**, 596 (1982).
[38] J. V. Prodan, W. D. Phillips, and H. Metcalf, Phys. Rev. Lett. **49**, 1149 (1982).
[39] T. E. Wall, J. F. Kanem, J. J. Hudson, B. E. Sauer, D. Cho, M. G. Boshier, E. A. Hinds, and M. R. Tarbutt, Phys. Rev. A **78**, 062509 (2008).
[40] X. Zhuang, A. Le, T. C. Steimle, N. E. Bulleid, I. J. Smallman, R. J. Hendricks, S. M. Skoff, J. J. Hudson, B. E. Sauer, E. A. Hinds, and M. R. Tarbutt, Phys. Chem. Chem. Phys. **13**, 19013 (2011).
[41] N. Wells and I. C. Lane, Phys. Chem. Chem. Phys. **13**, 19018 (2011).
[42] M. A. Chieda and E. E. Eyler, Phys. Rev. A **84**, 063401 (2011).
[43] L. Carr, D. DeMille, R. Krems, and J. Ye, New J. Phys. **11**, 055049 (2009).
[44] D. J. Berkeland and M. G. Boshier, Phys. Rev. A **65**, 033413 (2002).
[45] J. F. Barry, E. S. Shuman, and D. DeMille, Phys. Chem. Chem. Phys. **13**, 18936 (2011).
[46] N. R. Hutzler, M. F. Parsons, Y. V. Gurevich, P. W. Hess, E. Petrik, B. Spaun, A. C. Vutha, D. DeMille, G. Gabrielse, and J. M. Doyle, Phys. Chem. Chem. Phys. **13**, 18976 (2011).
[47] N. R. Hutzler, H.-I. Lu, and J. M. Doyle, ArXiv e-prints (2011), arXiv:1111.2841 [physics.atom-ph].
[48] D. Patterson and J. M. Doyle, J. Chem. Phys. **126**, 154307 (2007).
[49] D. Patterson, J. Rasmussen, and J. M. Doyle, New J. Phys. **11**, 055018 (2009).
[50] H.-I. Lu, J. Rasmussen, M. J. Wright, D. Patterson, and J. M. Doyle, Phys. Chem. Chem. Phys. **131**, 18986 (2011).
[51] M. Zhu, C. W. Oates, and J. L. Hall, Phys. Rev. Lett. **67**, 46 (1991).
[52] J. V. Prodan and W. D. Phillips, Prog. Quant. Electr. **8**, 231 (1984).
[53] S. Y. T. van de Meerakker, R. T. Jongma, H. L. Bethlem, and G. Meijer, Phys. Rev. A **64**, 041401 (2001).
[54] J. Riedel, S. Hoekstra, W. Jger, J. Gilijamse, S. van de Meerakker, and G. Meijer, Eur. Phys. J. D **65**, 161 (2011).
[55] C. H. Raymond Ooi, K.-P. Marzlin, and J. Audretsch, Eur. Phys. J. D **22**, 259 (2003).
[56] M. Falkenau, V. V. Volchkov, J. Rührig, A. Griesmaier, and T. Pfau, Phys. Rev. Lett. **106**, 163002 (2011).
[57] J. Stuhler, P. O. Schmidt, S. Hensler, J. Werner, J. Mlynek, and T. Pfau, Phys. Rev. A **64**, 031405 (2001).
[58] D. DeMille, D. R. Glenn, and J. Petricka, Eur. Phys. J. D **31**, 375 (2004).
[59] E. R. Meyer and J. L. Bohn, Phys. Rev. A **83**, 032714 (2011).